Wavelet Analysis and Applications
Tao Qian, Mang I. Vai and Xu Yuesheng, Eds.
Applied and Numerical Harmonic Analysis, 543–559

Detection of Spindles in Sleep EEGs Using a Novel Algorithm Based on the Hilbert-Huang Transform

Zhihua Yang, Lihua Yang and Dongxu Qi

Abstract. A novel approach for detecting spindles from sleep EEGs (electroencephalograph) automatically is presented in this paper. Empirical mode decomposition (EMD) is employed to decompose a sleep EEG, which are usually typical nonlinear and non-stationary data, into a finite number of intrinsic mode functions (IMF). Based on these IMFs, the Hilbert spectrum of the EEG can be calculated easily and provides a high resolution time-frequency presentation. An algorithm is developed to detect spindles from a sleep EEG accurately, experiments of which show encouraging detection results.

Mathematics Subject Classification (2000). Primary 94A13; Secondary 42A16.

Keywords. Empirical mode decomposition, Hilbert-Huang transform, signal detection.

1. Introduction

Sleep is a complicated physiological process. Research on sleep is very important to both clinical diagnosis and curative effect evaluation in nervous psychiatry. Generally, sleep consists of two phases: no-rapid eye movement (NREM) and rapid eye movement(REM). The NREM phase can be decomposed into 4 stages according to sleep depths [6]. A crucial clue for the sleep depth to be at the second or the third stages is that the sleep-spindles, whose frequencies are between 12 and 20Hz, take place in the EEG (electroencephalo-graph) [7].

Traditionally, sleep-spindles are detected visually by neurologists or sleep experts. Research on automated sleep analysis can be traced back to as early as the 1970s [12, 13, 9, 11, 2, 8, 10, 5]. In recent years, two novel algorithms for automated

This work was supported by NSFC (Nos. 60475042, 60133020), the National Key Basic Research Project of China (No.2004CB318000) and the Scientific and Technological Planning Project of Guangzhou city.

detection of spindles in sleep EEG were developed by using classical time-frequency analysis [7, 3]. Since EEGs are typically nonlinear and non-stationary signals and the duration of a sleep-spindle is usually very short, it is usually difficult to obtain satisfactory results in automated detection of sleep-spindles by using traditional time-frequency analysis.

Recently, a novel analysis method for nonlinear and non-stationary data, which is called *Hilbert-Huang Transform (HHT)*, was developed [4]. Its key part is the so-called *empirical mode decomposition (EMD)*, with which any complicated data set can be decomposed into a finite and often small number of *intrinsic mode function(IMF)* that admit well-behaved Hilbert transforms. EMD is adaptive, and therefore, highly efficient. It is based on the local characteristic time scale of the data and is applicable to nonlinear and non-stationary processes. With the Hilbert transform, the IMFs yield instantaneous frequencies as functions of time that give sharp identifications of embeded structures. The final presentation of the results is a time-frequency-energy distribution, designated as the Hilbert spectrum, which has high time-frequency localization.

Because of these properties, in this paper, HHT is employed to analyze sleep EEGs and an algorithm to detect spindles from sleep EEGs automatically is developed. Experiments show an encouraging detection rate which is higher than those developed in [7, 3].

This paper is organized as follows: Section 2 is a brief summary on the Hilbert-Huang Transform; Analysis of EEG data based on HHT is given in Section 3; In Section 4, a novel algorithm for automated detection of sleep-spindles is proposed. Experiments to support the algorithm are conducted and the anti-noise ability is discussed in Section 5; Finally, Section 6 is the conclusion of this paper.

2. Hilbert-Huang Transform

The Hilbert-Huang Transform (HHT) was proposed by Huang et al [4]. It consists of two parts: (1) *Empirical Mode Decomposition (EMD)*, and (2) *Hilbert Spectral Analysis*. With EMD, any complicated data set can be decomposed into a finite and often small number of *intrinsic mode functions (IMF)*. An IMF is defined as a function satisfying the following conditions:

(a) The number of extrema and the number of zero-crossings must either be equal or differ at most by one;
(b) At any point, the mean value of the envelope defined by the local maxima and the envelope defined by the local minima is zero.

An IMF defined as above admits well-behaved Hilbert transforms. EMD decomposes signals adaptively and is applicable to nonlinear and non-stationary data (Fundamental theory on nonlinear time series can be found in [1]). In this section, a brief introduction is given to make this paper somewhat self-contained. The readers are referred to [4] for details.

For an arbitrary function $X(t)$ in L_p-class [14], its Hilbert transform $Y(t)$ is defined as

$$Y(t) = \frac{1}{\pi} P \int_{-\infty}^{\infty} \frac{X(t')}{t - t'} \mathrm{d}t', \tag{2.1}$$

where P indicates the Cauchy principal value. Consequently an analytic signal $Z(t)$ can be produced by

$$Z(t) = X(t) + iY(t) = a(t)e^{i\theta(t)}, \tag{2.2}$$

where

$$a(t) = [X^2(t) + Y^2(t)]^{\frac{1}{2}}, \ \theta(t) = \arctan(\frac{Y(t)}{X(t)}) \tag{2.3}$$

are the instantaneous amplitude and the phase of $X(t)$. Since the Hilbert transform $Y(t)$ is defined as the convolution of $X(t)$ and $1/t$ by Eq. (2.1), it emphasizes the local properties of $X(t)$ even though the transform is global. In Eq. (2.2), the polar coordinate expression further clarifies the local nature of this representation. With Eq. (2.2), the instantaneous frequency of $X(t)$ is defined as

$$\omega(t) = \frac{d\theta(t)}{dt}. \tag{2.4}$$

However, there is still considerable controversy on this definition. A detailed discussion and justification can be found in [4].

EMD is a necessary pre-processing of the data before the Hilbert transform is applied. It reduces the data into a collection of IMFs and each of them represents a simple oscillatory mode that is a counterpart of a simple harmonic function, but is much more general. With this definition, one can decompose any function according to the following algorithm.

Algorithm 2.1. Let $X(t)$ be a signal.

Step 1 Initialize: $r_0(t) = X(t), \ i = 1$;

Step 2 Extract the i-th IMF as follows:

- **(a)** Initialize: $h_0(t) = r_{i-1}(t), \ j = 1$;
- **(b)** Extract the local minima and maxima of $h_{j-1}(t)$;
- **(c)** Interpolate the local maxima and the local minima by cubic splines to form $u_{j-1}(t)$ and $l_{j-1}(t)$ as the upper and lower envelops of $h_{j-1}(t)$ respectively;
- **(d)** Calculate $m_{j-1}(t) = \frac{u_{j-1}(t)+l_{j-1}(t)}{2}$ as an approximation of the local mean of $h_{j-1}(t)$ at t;
- **(e)** Let $h_j(t) = h_{j-1}(t) - m_{j-1}(t)$;
- **(f)** If the stopping criterion is satisfied, i.e., $h_j(t)$ is an IMF, set $\mathrm{imf}_i(t) = h_j(t)$; Else go to (b) with $j = j + 1$.

Step 3 Let $r_i(t) = r_{i-1}(t) - \mathrm{imf}_i(t)$;

Step 4 If $r_i(t)$ still has at least 2 extrema, go to Step 2 with $i = i + 1$; otherwise the decomposition is finished and $r_i(t)$ is the residue.

By Algorithm 2.1, any signal $X(t)$ can be decomposed into finite IMFs, $\mathrm{imf}_j(t)$ $(j = 1, \cdots, n)$, and a residue $r(t)$, where n is nonnegative integer depending on $X(t)$, i.e.,

$$X(t) = \sum_{j=1}^{n} \mathrm{imf}_j(t) + r(t). \tag{2.5}$$

For each $\mathrm{imf}_j(t)$, let $X_j(t) = \mathrm{imf}_j(t)$. Its corresponding instantaneous amplitude $a_j(t)$ and instantaneous frequency $\omega_j(t)$ can be computed with Eqs. (2.3) and (2.4). By Eqs. (2.2) and (2.4), $\mathrm{imf}_j(t)$ can be expressed as the real part, Re, in the following form:

$$\mathrm{imf}_j(t) = \mathrm{Re}\left[a_j(t) \exp\left(i \int \omega_j(t) dt\right)\right]. \tag{2.6}$$

Therefore, by Eqs. (2.5) and (2.6), $X(t)$ can be expressed as the IMF:

$$X(t) = \mathrm{Re} \sum_{j=1}^{n} a_j(t) \exp\left(i \int \omega_j(t) dt\right) + r(t). \tag{2.7}$$

It is interesting to compare the representation above with the following classical Fourier expansion:

$$X(t) = \sum_{j=1}^{\infty} a_j e^{i\omega_j t}, \tag{2.8}$$

where both a_j and ω_j are constants. Contrasting Eq. (2.7) with Eq. (2.8), it is apparent that the IMF expansion provides a generalized Fourier expansion. It relieves the restriction of the constant amplitude and fixed frequency of Fourier expansion, and arrives at a variable amplitude and frequency representation. With the IMF expansion, the amplitude and frequency modulations are clearly separated. Its main advantage over Fourier expansion is that it accommodates nonlinear and non-stationary data perfectly.

Equation (2.7) enables us to represent the amplitude and the instantaneous frequency as functions of time in a three-dimensional plot, in which the amplitude is contoured on the time-frequency plane. The time-frequency distribution of amplitude is designated as the Hilbert amplitude spectrum or simply Hilbert spectrum, denoted by $H(\omega, t)$. It can also be defined equivalently in mathematics as follows: Let $X(t)$ be decomposed into finite IMFs $\mathrm{imf}_j(t)$ $(j = 1, \cdots, n)$ and a residue $r(t)$ by Algorithm 2.1, then,

$$H(\omega, t) = \begin{cases} 0 & \text{if } J_{\omega,t} \text{ is an empty set,} \\ \sum_{j \in J_{\omega,t}} a_j(t), & \text{otherwise,} \end{cases} \tag{2.9}$$

where $J_{\omega,t} = \{j | 0 \le j \le n \text{ satisfying } \omega_j(t) = \omega\}$.

$H(\omega, t)$ gives a time-frequency-amplitude distribution of a signal $X(t)$. If amplitude squared is more desirable commonly to represent energy density, then the squared values of amplitude can be substituted to produce the Hilbert energy spectrum.

3. HHT for EEG Data

To observe the performance of the HHT for EEG data, a 6 second segment, denoted by $X(t)$, is selected from a sleep EEG which is sampled when the sleep is at the 2nd stage of a NREM phase. It contains two sleep-spindles, marked by 'A' and 'B' respectively, as shown in Fig.1. With Algorithm 2.1, it is decomposed into seven IMFs and a residue, which are shown in Fig. 2(c1) $\sim$ (c8) respectively from top to bottom. From Fig.2(c2), it is easy to see that there are two sub-segments of high amplitude in the periods from about 20 to 160 and from about 750 to 1050 respectively, whose frequencies are around 13Hz (the first consists of about 9 waves within 0.7s(140 points) and the second consists of 18 waves within 1.5s(300 points)). Such a sub-segment whose amplitude is high and frequency is between 12 $\sim$ 20Hz is a possible spindle wave we want to detect, which is called a *PSW* for simplicity. Based on the analysis of this example, it seems possible to detect sleep-spindles based on features in some of the IMFs, such as the second one shown in Fig.2(c2). To examine the observation, let us consider another example as shown in Fig.3. It is also a sleep EEG segment of 6 seconds, in which only one sleep-spindle, marked by 'A', is included. Similarly, with Algorithm 2.1, it is decomposed into seven IMFs and a residue, which are shown in Fig. 4(c1) $\sim$ (c8) respectively from top to bottom. It is observed that the second IMF does not contain PSWs. However, in the third IMF as shown in Fig.4(c3), there is a PSW starting at about the 800 and ending at the 1000 (corresponding the part marked by 'A' in Fig.3). By conducting more experiments like Fig.2 and Fig.4, we conclude that, for a sleep EEG segment which contains spindles, in general, one cannot determine in which IMF the interesting sub-segments may appear. In fact, a spindle consists of a number of oscillatory modes which are the same or similar in local characteristic time scale (an oscillatory mode is a wave between a pair of successive maxima or a pair of successive minima [4]), when a EEG segment is decomposed by EMD, these oscillatory modes may be dispersed to different IMFs. Therefore, the PSWs cannot be detected based on some IMFs and consequently

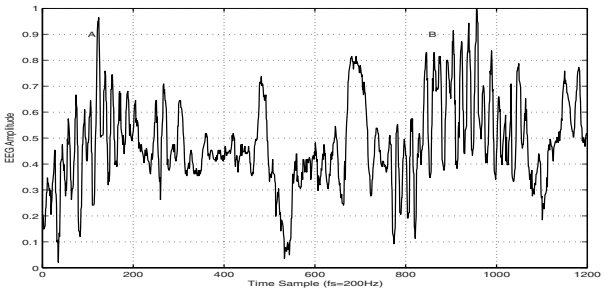

FIGURE 1. A sleep EEG segment of 6 seconds at the second sleep stage, in which two sleep-spindles are included as marked by 'A' and 'B' respectively.

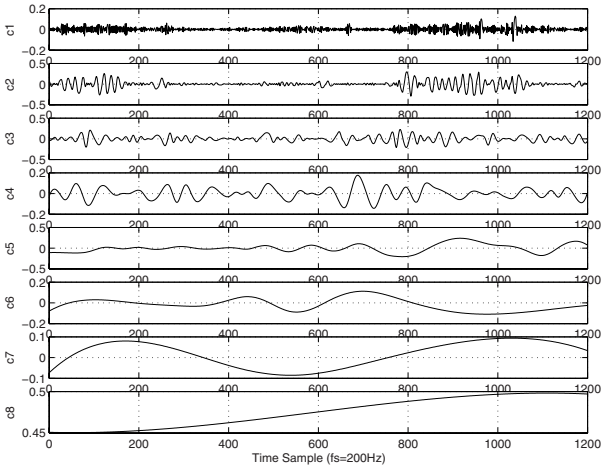

FIGURE 2. The resulting EMD components from the EEG data of Fig. 1. The last component, c8, is not an IMF, it is the residue.

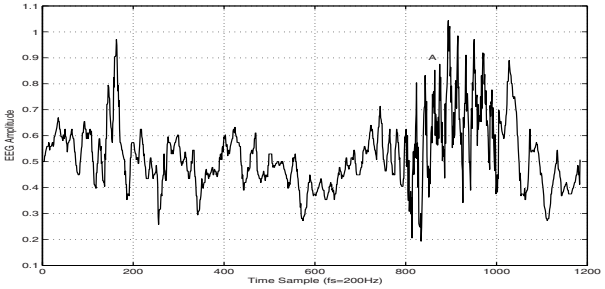

FIGURE 3. A sleep EEG segment of 6 seconds long at the second sleep stage, in which a sleep-spindle is included as marked by 'A'.

the Hilbert spectrum, which is the global time-frequency-energy distribution, is considered as a natural substitution for the detection of sleep-spindles from EEGs.

Since IMFs have good time-frequency resolution as described in Section 2 (see [4]), one can predict that, in the Hilbert spectrum of a sleep EEG segment, high energies will take place within its PSWs. This prediction is verified by the graphs of the Hilbert spectrum of the sleep EEG segments: Fig. 5 and Fig. 6 are respectively the contour maps of the Hilbert spectrums of the sleep EEG segments shown in Fig. 1 and Fig. 3. In Fig. 5, one can find two high energy bands whose frequencies are $8 \sim 20$Hz or so: one starts at about 0 and ends at 200, the other starts at about 750 and ends at 1050, as highlighted by the two rectangles in the figure. Similarly, in Fig. 6, there is a high energy band whose frequencies are 8 $\sim$ 20Hz or so, starting at about 730 and ending at 1000, as highlighted by the

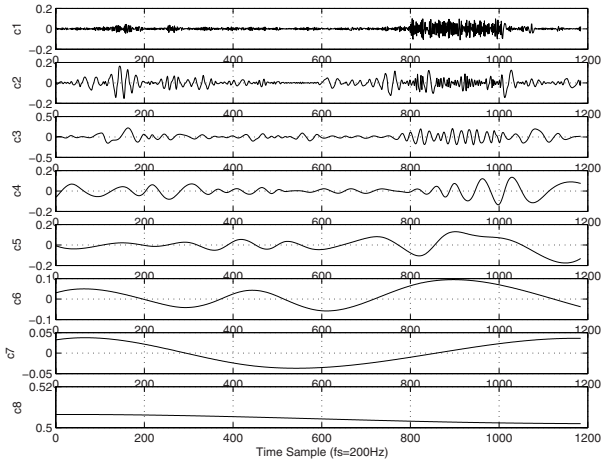

FIGURE 4. The resulting EMD components from the EEG data of Fig. 3. The last component, c8, is not an IMF, it is the residue.

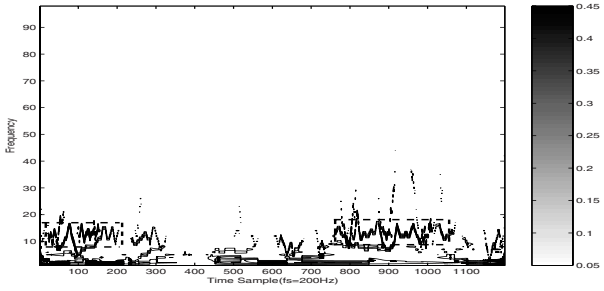

FIGURE 5. The contour map of Hilbert spectrum for the EEG data of Fig. 1.

rectangle in Fig. 6. Therefore, the locations and durations of the sleep-spindles can be detected from the Hilbert spectrum of sleep EEGs successfully.

4. A Novel Algorithm for Automated Detection of Sleep-Spindles

In this section, an auto-detection algorithm for sleep-spindle detection is developed and, consequently, experiments are conducted to support the algorithm.

Based on the discussion above and the fact that the duration of a sleep-spindle is usually longer than 0.5s in practice, a novel method for automated detection of spindles from a EEG is developed in this section.

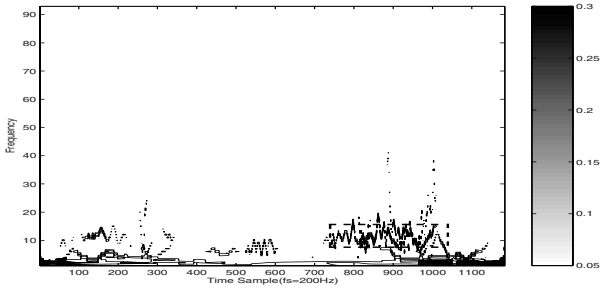

FIGURE 6. The contour map of Hilbert spectrum for the EEG data of Fig. 3.

In practice, a sleep EEG contains a large amount of data. It is terribly time-consuming to calculate the Hilbert spectrum of a global sleep EEG signal. Experiments show that the time needed for calculating the Hilbert spectrum, which is called the CPU time hereafter for simplicity, does not depend linearly on the data length of the signal. When the length of data is longer than 1500 or so, the CPU time needed increases rapidly. The five dotted curves in Fig. 7 illustrates how the CPU times depend on the datum lengths for five signals of 2000 random data ranging from 0 to 1, when a PC of Pentium IV-1.7GHz is used. It should be pointed out that the graph changes somewhat if the signals is replaced by another signal.

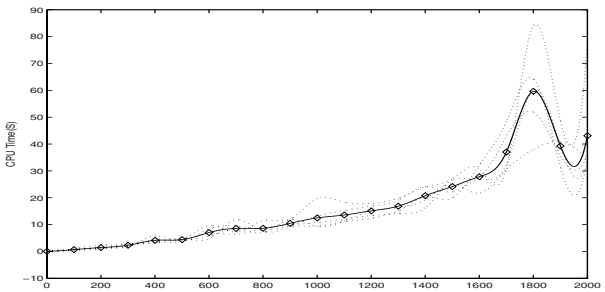

FIGURE 7. CPU time as a function of the length of the data set

The solid curve in Fig. 7 is the average of the five dotted curves, which illustrates how the CPU time depends on the datum length in the rough. Thus, to save CPU time, a global EEG signal should be divided into many short segments. The length of the short segments should be as long as possible to keep enough integrality of data if the CPU time is acceptable. According to Fig. 7, it is a reasonable tradeoff to divide the global EEG signal into segments of $1200 \sim 1600$ data (about $6 \sim 8$ seconds for frequency of sampling = 200Hz). In our experiments, the global sleep EEG is divided into segments of 1200 data points. The corresponding time for each segment is about 6 seconds.

After a sleep EEG is divided as before, we decompose each segement with EMD into IMFs. Since the first IMF usually consists of the highest frequency components of the segment, such as noise (see Fig. 2(c1) and Fig. 4(c1)), it is discarded in our algorithm. For each segment, the sleep-spindles are detected by the following algorithm.

Algorithm 4.1. Let $x(t)$ be a segment of data of length 1200. The sleep-spindles are detected as follows:

Step 1 Decompose $x(t)$ with EMD into IMFs, then remove the first IMF. For each other IMF, calculate its instantaneous frequency and instantaneous amplitude by Eqs. (2.4) and (2.3). Quantify the instantaneous frequency into integers between 1 and 100Hz.

Step 2 Compute the Hilbert spectrum $H(\omega, t)$; here it is a matrix of 100 rows and 1200 columns. Then normalize the amplitude of $H(\omega, t)$ linearly such that the values of $H(\omega, t)$ range from 0 to 255.

Step 3 Extract the 8th to 20th rows of $H(\omega, t)$ to form a sub-matrix, denoted by M, of 13 rows and 1200 columns.

Step 4 Calculate the maximum of each column of M to generate an array, $C = (C[1], \cdots, C[1200])$. It is an energy measure of the data on frequencies ranging from $8 \sim 20$Hz at each local time. Then, define a smoothed version of C as:

$$C_1[k] = \frac{1}{L} \sum_{i=k-L/2}^{k+L/2} C[i],$$

where L, an even integer, is the width of the smoothing window ($L = 50$ in the experiments of this paper) and the boundary extension is conducted as: $C[i] = C[1]$ for $i \leq 0$ and $C[i] = C[1200]$ for $i > 1200$.

Step 5 Let T be a threshold. Then, we search $1 \leq k \leq 1100$ and $I \geq 100$ such that

$$C_1[k + i - 1] \geq T \text{ for } i = 1, 2, \cdots, I,$$

and

$$C_1[k + I] < T \text{ or } k + I = 1200.$$

Then a sleep-spindle that starts at k and has duration I is detected. We set $T = 50$ in the experiments of this paper.

5. Experiments

In this section, experiments are conducted to support our algorithm on sleep-spindle detection.

For the segment of a sleep EEG shown in Fig. 1, according to Steps 1 and 2 of Algorithm 4.1, its IMFs and Hilbert spectrum $H(\omega, t)$ are calculated as shown in Figs. 2 and 5 respectively. By Step 3 of Algorithm 4.1, the sub-matrix M of the 8th to 20th rows of $H(\omega, t)$ is generated as shown in Fig. 8. Then the energy array

C of M and the smoothed version, C_1, are calculated in accordance with Step 4 of Algorithm 4.1, which are shown in Fig. 9: the top is C and the bottom is C_1. Finally, by Step 5, two spindles of a sleep EEG are detected in this segment as shown in Fig. 10, in which the starting points, the durations, and the end points are marked by the dotted lines. The first starts at about the 20th datum (namely: the 0.1th second) with a duration of about 0.8s and the second starts at about the 750th datum (namely: the 3.75th second) with a duration of about 1.5s.

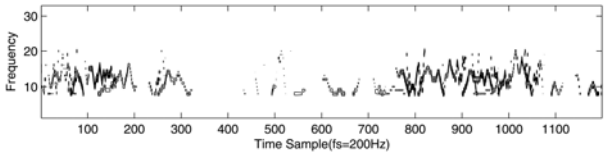

FIGURE 8. The sub-matrix M generated by the 8th – 20th rows of the Hilbert spectrum $H(\omega, t)$ shown in Fig. 5

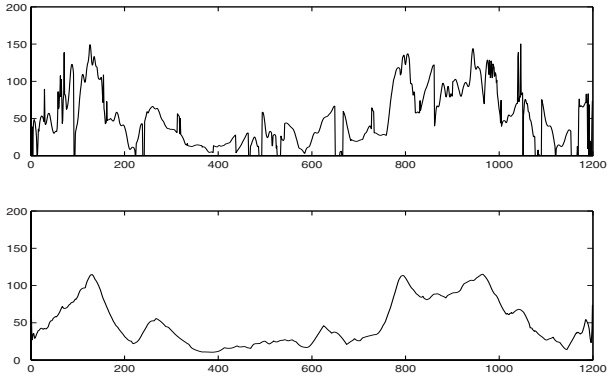

FIGURE 9. The top: The energy array of M shown in Fig. 8, C, each of whose component is the maximum of the elements in the corresponding column of M. The bottom: The smoothed version C_1 of C calculated according to Step 4 of Algorithm 4.1.

Similarly, Figs. 4 and 6 are the IMFs and the contour map of the Hilbert spectrum $H(\omega, t)$ of the segment shown in Fig. 3 in accordance with Steps 1 and 2 of Algorithm 4.1. The corresponding sub-matrix M calculated by Step 3 are shown in Fig. 11. Then, the energy array C of M and the smoothed version, C_1, calculated by Step 4, are displayed graphically in Fig. 12: the top is C and the bottom is C_1. Fig. 13 is the detection result by Step 5, in which a sleep-spindle is detected and marked with dotted lines. It starts at about the 750th datum (namely: the 3.75th second) with a duration of about 1.25s.

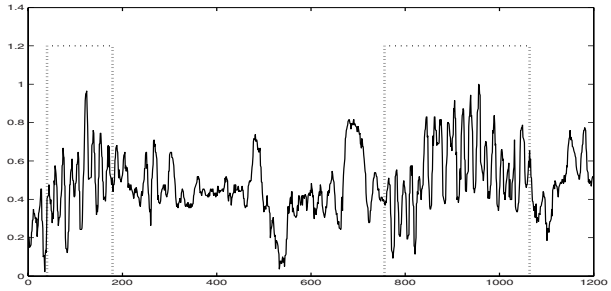

FIGURE 10. The detection result for the segment in Fig. 1. Two sleep-spindles are detected and marked with dotted lines. The first starts at about the 20th datum (namely: the 0.1th second) with a duration of about 0.8s and the second starts at about the 750th datum (namely: the 3.75th second) with a duration of about 1.5s.

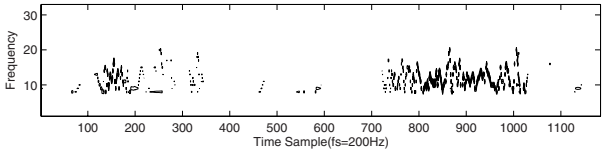

FIGURE 11. The sub-matrix M generated by the 8th – 20th rows of the Hilbert spectrum $H(\omega, t)$ shown in Fig. 6

To test our detection algorithm, 100 segments, each of which consists of 1200 data (about 6 seconds with frequency of sampling 200Hz) and all of which contain 183 spindles, are selected from a sleep EEG database. The locations and durations of these sleep-spindles have been determined visually by experts. For an automated detection algorithm, its detection accuracy depends on two aspects: (1) the accuracy of the location detected and (2) the accuracy of the duration detected. To estimate them quantitatively, a mis-detection degree is introduced as follows.

Definition 5.1. Let X(t) be a sleep EEG segment which contains a sleep-spindle starting at t_b and ending at t_e. For an automated detection method for sleep-spindles, the mis-detection degree, simply denoted by MD, is defined as follows:

1. if one sleep spindle is detected from X(t), with starting point t'_b and end point t'_e, then
$$MD = \frac{L_\vee - L_\wedge}{L}, \tag{5.1}$$
where, $L_\vee = \max(t_e, t_e^{'}) - \min(t_b, t_b^{'})$, $L_\wedge = \min(t_e, t_e^{'}) - \max(t_b, t_b^{'})$ and $L = t_e - t_b$ as shown in Fig. 14.
2. if no spindle or more than one spindle is/are detected, then $MD = \infty$.

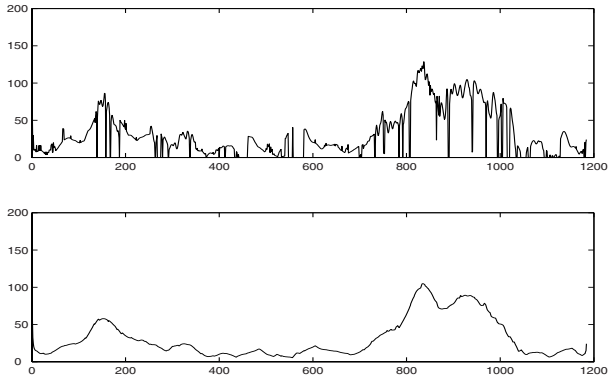

FIGURE 12. The top: The energy array of M, shown at the bottom of Fig. 11, denoted by C, each of whose component is the maximum of the elements in the corresponding column of M. The bottom: The smoothed version C_1 of C calculated according to Step 4 of Algorithm 4.1.

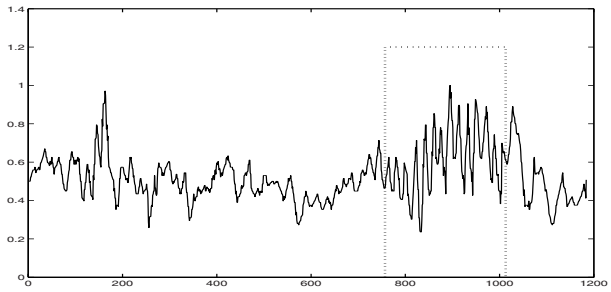

FIGURE 13. The detection result for the segment in Fig. 3. A sleep-spindle is detected and marked with dotted lines, which starts at about the 750th datum (namely: the 3.75th second) with a duration of about 1.25s.

It is easy to see that MD is a nonnegative number and MD=0 if and only if the sleep-spindle is detected accurately, and the smaller MD is, the more accurately the detection does. Table 1 lists the distribution of the MDs produced by Algorithm 4.1 for all the 183 samples and the corresponding histogram is displayed in Fig. 15, in which all the MDs greater than 1 is included into that of MD=1.1. It is encouraging to see that most of the MDs are between 0 and 0.2, which shows that our algorithm arrives at satisfying detection results in both locations and durations.

Let us compare our technique with those in [3, 7]. The same dataset is employed to conduct the experiments. The distributions of the corresponding MDs

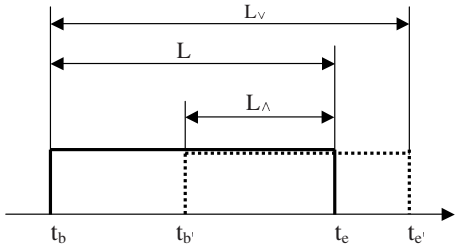

FIGURE 14. $L_\vee, L_\wedge$ and L in Definition 2

TABLE 1. The distribution of the MDs produced by Algorithm 4.1, NS is the number of spindles whose MDs are within the given interval.

MD	0 ∼0.1	0.1 ∼0.2	0.2 ∼0.3	0.3 ∼0.4	0.4 ∼0.5	0.5 ∼0.6	0.6 ∼0.7	0.7 ∼0.8	0.8 ∼0.9	0.9 ∼1	> 1
NS	1101	443	86	51	43	25	17	7	3	3	51

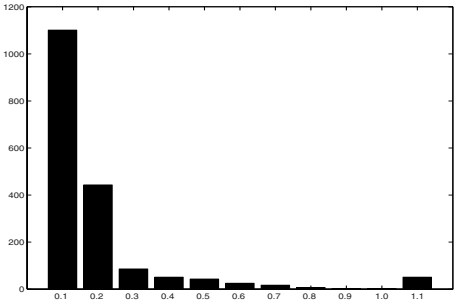

FIGURE 15. The histogram of the MDs corresponding to Table 1

calculated according to the algorithms in [7] and [3] are listed in the 3th and 4th rows of Table 2 respectively. To compare more conveniently, the distribution of the MDs by our algorithm is also listed in the 2nd row of Table 2. The corresponding histogram is shown in Fig. 16, in which all the MDs greater than 1 is included into that of MD=1.1. It is noticed that the MDs produced by our algorithm concentrate much closer to 0 than those by [3] and [7], which implies that our detection does better than theirs. To describe the detection result quantitatively, we define the detection rate as the ratio of the number of MDs which are less than some given threshold, T, to the total number of spindles. With this definition and $T = 0.2, 0.5$ and 1 respectively, the detection rates according to Algorithm 4.1, the algorithms in [7] and [3] are listed in Table 3.

Before the end of this section, let us discuss the detection of spindles from noisy sleep EEGs by Algorithm 4.1. It is easy to understand that Algorithm 4.1

TABLE 2. The distributions of the MDs calculated according to Algorithm 4.1, the algorithms in [7] and [3]. NS_j are the numbers of spindles whose MDs are within the given intervals, with j=1, 2, and 3 corresponding to Algorithm 4.1, the algorithms in [7] and in [3] respectively.

MD	0 ∼0.1	0.1 ∼0.2	0.2 ∼0.3	0.3 ∼0.4	0.4 ∼0.5	0.5 ∼0.6	0.6 ∼0.7	0.7 ∼0.8	0.8 ∼0.9	0.9 ∼1	> 1
NS_1	1101	443	86	51	43	25	17	7	3	3	51
NS_2	893	466	164	88	42	23	12	9	11	9	113
NS_3	752	367	231	97	44	48	26	12	10	13	230

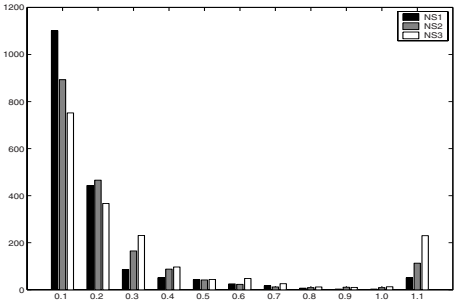

FIGURE 16. The histogram of the MDs corresponding to Table 2

TABLE 3. The detection rates corresponding to Algorithm 4.1, the algorithms in [7] and [3] for $T = 0.2, 0.5$ and 1

Detection rate	$T = 0.2$	$T = 0.5$	$T = 1$
Algorithm 4.1	84.4%	94.2%	97.2%
Algorithm in [7]	74.3%	90.3%	93.8%
Algorithm in [3]	61.1%	81.5%	87.4%

can do well for noisy sleep EEG signals since the frequencies of sleep spindles, about 13Hz, are usually much lower than those of noise. Another reason for this anti-noise ability is that the first IMF has no contribution to the Hilbert spectrum. To demonstrate our view, a great number of experiments have been conducted and excellent results are obtained. Fig. 17 are three noisy versions of Fig. 3 by adding Gaussian white noises with SNR (Signal Noise Ratio, which is defined as the ratio of signal variance to noise variance in dB.) 20dB, 25dB and 30dB respectively from top to bottom. The detection results are shown in Fig. 18, corresponding to those in Fig. 17 from top to bottom. It is easy to see that, spindles can be detected successfully with a minor change in the locations and durations even though the SNRs are very low.

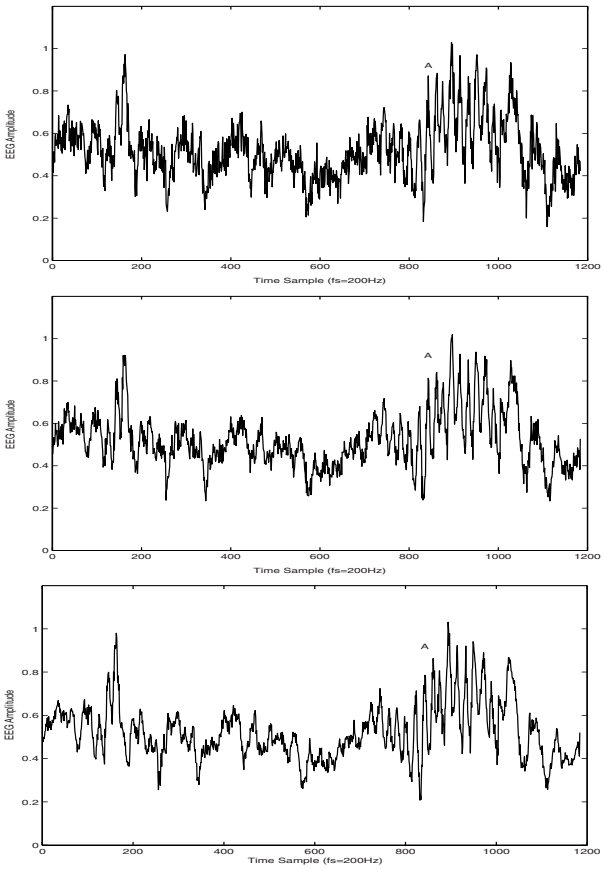

FIGURE 17. Three noisy versions of Fig. 3 by adding Gaussian white noises with SNR 20, 25 and 30 respectively from top to bottom.

6. Conclusion

In this paper, a novel approach for detecting spindles automatically from a sleep EEG based on the Hilbert-Huang transform is developed. Empirical mode decomposition is employed to decompose sleep EEGs into a finite and often small number of intrinsic mode functions. Then the Hilbert spectrum $H(\omega, t)$ is used to give a high resolution time-frequency presentation and extract features of EEGs. Consequently, an algorithm is proposed to detect spindles automatically from a sleep EEG. Experiments show more accurate detection results than those in [7, 3]. Finally, the anti-noise ability of the algorithm is demonstrated theoretically and experimentally.

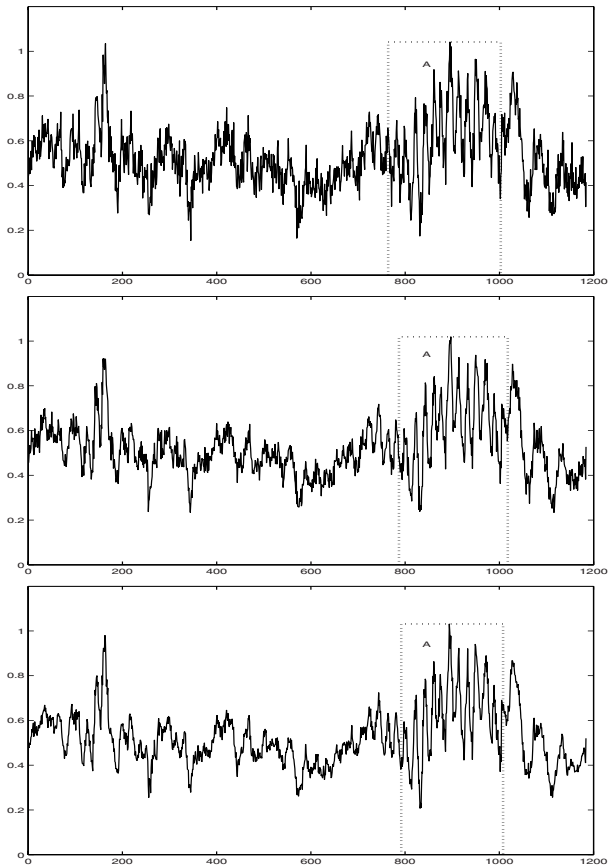

FIGURE 18. The detection results of Fig. 17 correspondingly from top to bottom by Algorithm 4.1

References

[1] Hongzhi An and Min Chen. *Non-linear Time series Analysis*. Shanghai Science & Technology Press, China, 1998.

[2] J. Doman, C. Detka, and T. Hoffman et al. Automating the sleep laboratory: Implementation and validation of digital recording and analysis. *International Journal of Biomedical Computing*, 38(3):277–290, 1995.

[3] Fei Huang and Chongxun Zheng. Automated recognition of spindles in sleep electroencephalogram base on time-frequency analysis. *Journal of Xi'An Jiao Tong University*, 36(2):218–220, 2002.

[4] N. E. Huang, Z. Shen, and S. R. Long et al. The empirical mode decomposition and the Hilbert spectrum for nonlinear and non-stationary time series analysis. *Proceedings of the Royal Society of London*, A(454):903–995, 1998.

[5] M. J. Korenberg. A robust orthogonal algorithm for system identification and time-series analysis. *Biological Cybernetics*, 60:267–276, 1989.

[6] Leukel. *Essential of Physiological Psychology*. The CV Company, USA, 1978.

[7] Jianping Liu, Shiyong Yang, and Chongxun Zheng. High resolution time-frequency analysis method for extracting the sleep spindles. *Journal of Biomedical Engineering*, 17(1):50–55, 2000.

[8] N. Pradhan and P. K. Sadasivan. The nature of dominant lyapunov exponent and attractor dimension curve of eeg in sleep. *Computers in Biology and Medicine*, 26(5):419–428, 1996.

[9] J. Pricipe, S. K. Gala, and T. G. Chang. Sleep staging automation base on the theory of evidence. *IEEE Transactions on Biomedical Engineering*, 36(5):503–509, 1987.

[10] Shannahoff-Khalsa David S., Gillin J. Christian, and etc. Ultradian rhythms of alternating cerebral hemispheric eeg dominance are coupled to rapid eye movement and non-rapid eye movement stage 4 sleep in humans. *Sleep Medicine*, 2(4):333–346, 2001.

[11] N. Schaltenbrand, R. Lengelle, and J. P. Macher. Neural network model: Application to automatic analysis of human sleep. *Computer and Biomedical Research*, 26(2):157–171, 1993.

[12] J. R. Smith, I. Karacan, and M. C. K. Yang. Automated analysis of the human sleep EEG. *Waking and Sleeping*, 2:229–237, 1978.

[13] E. Stanus, B. Lacroix, and M. Kerkhofs et al. Automated sleep coring: A comparative reliability study of two algorithms. *Electroencephalography and Clinical Neurophysiology*, 66(4):448–454, 1987.

[14] E. C. Titchmarsh. *Introduction to the Theory of Fourier Integrals*. Oxford University Press, 1948.

Zhihua Yang
Information Science School
GuangDong University of Business Studies,
Guangzhou 510320, P. R. China
e-mail: yangyangzh@tom.com

Lihua Yang
School of Mathematics and Computing Science
Sun Yat-sen University, Guangzhou 510275, P. R. China
e-mail: mcsylh@mail.sysu.edu.cn

Dongxu Qi
Faculty of Information Technology
Macao University of Science and Technology, Macao

School of Information Science and Technology
Sun Yat-sen University, Guangzhou 510275, P. R. China
e-mail: dxqi@must.edu.mo